# ARTICLES

## Short range interaction of nucleons inside the nucleus via $^4$He$(e,e'p)R$ reactions

J.M. Le Goff,[1] M. Bernheim,[1] M.K. Brussel,[2] G.P. Capitani,[3] J.F. Danel,[1]
E. De Sanctis,[3] S. Frullani,[4] F. Garibaldi,[4] A. Gerard,[1] M. Jodice,[4]
A. Magnon,[1] C. Marchand,[1] J. Morgenstern,[1] J. Picard,[1] D. Reffay,[1]
P. Vernin,[1] and A. Zghiche[1]

[1]*Service de Physique Nucléaire (SPhN), CEN Saclay, F-91191 Gif-sur-Yvette Cedex, France*
[2]*Department of Physics, University of Illinois at Urbana Champaign, Urbana, Illinois 61801*
[3]*Laboratori Nazionali di Frascati, Istituto Nazionale di Fisica Nucleare, I-00044 Frascati, Italy*
[4]*Laboratori di Fisica, Istituto Superiore di Sanitá*
*and Istituto Nazionale di Fisica Nucleare, Sezione Sanitá I-00161 Roma, Italy*

(Received 19 May 1994)

Cross sections for the $^4$He$(e,e'p)R$ reaction have been measured for recoil momenta between 225 and 500 MeV/$c$. We find (1) that in the continuum channel a peak in the missing energy spectrum appears which shifts with increasing recoil momentum in a predictable way, and (2) that for the highest recoil momenta (above 300 or 350 MeV/$c$) overall agreement is obtained with microscopic calculations in which the scattering on nucleon pairs predominates. These results strongly suggest that the highest recoil momenta are generated by the scattering on one of a pair of nucleons. This interpretation is reinforced by an observed continuum momentum distribution which, for high recoil momenta, resembles the momentum distribution of deuterium. We infer that the high momentum part of the momentum distribution of a nucleon pair appears unmodified when embedded in a nuclear medium.

PACS number(s): 21.45.+v, 21.30.+y, 25.30.Fj

### I. INTRODUCTION

The independent particle shell model (IPSM) describes the nucleus as a collection of nucleons moving independently in the mean field generated by the other nucleons. The nucleons fill the resulting shells up to the Fermi energy. Such a model gives a quite good description of the one-body properties of nuclei. Experimentalists have studied these properties rather extensively, initially with hadronic probes in pickup, stripping, and knockout reactions where the cross sections are relatively large [1], and more recently with electromagnetic probes for which the reaction dynamics are more straightforward [2]. For instance the momentum distribution in the different shells have been measured, giving direct evidence for the validity of the independent particle shell model.

However, the IPSM is only a first order description, the nucleons are not fully independent, there are nucleon-nucleon correlations in the nuclear wave function, and the nucleus cannot be totally described by one-body properties. Considerable theoretical effort was involved in describing the two-body properties, but as yet there is little experimental information available on these properties and what exists so far is rather indirect. This is the case with $(e,e'p)$ experiments which attempted to measure occupation numbers, i.e., how much of the IPSM shell is actually filled. Orbitals of "closed shell" nuclei were found which did not appear to be completely filled, a result attributable to nucleon-nucleon correlations in the nuclear ground states.

The existence of multibody effects has been cited in the so-called "dip" region between the quasielastic peak and the $\Delta$-resonance peak of inclusive $(e,e')$ experiments. Such experiments showed an anomalously large transverse cross section, not explained in terms of independent nucleon processes alone. This region can be probed more meticulously with $(e,e'p)$ experiments. When the cross section for the $^{12}$C$(e,e'p)$ reaction was measured in the quasielastic region [3] it could be well explained in terms of proton (one-body) knockout from the $1p$ or $1s$ shells only. In contrast, in the dip region it showed additional contributions up to the highest missing energies measured, 150 MeV [4]. A separation of the transverse (magnetic) and longitudinal (Coulomb) parts of the $(e,e'p)$ cross section was also made [5]. The longitudinal part could be explained in terms of one-body knockout alone. However, the transverse part showed an excess yield above the two-particle emission threshold. Summarizing, a contribution which is not one body is observed [4,5]; it is present only in the transverse part of the cross section and then is probably due to the complex reaction mechanism involved rather than to the intrinsic ground state properties of the nuclei. Similar results have also been observed in real photon (transverse) experiments [6].

Inclusive $(e,e')$ experiments can in principle give rather model independent information about the two-body properties of the nuclear wave function [7, 8]. More pre-

 

cisely one can extract the proton-proton correlation function which is defined in terms of the $\rho$ and $\rho_2$ one-body and two-body density functions

$$c^{(2)}(\mathbf{q}) = \int e^{i\mathbf{q}\cdot(\mathbf{r}-\mathbf{r}')}[\rho_2(\mathbf{r},\mathbf{r}') - \rho(\mathbf{r})\rho(\mathbf{r}')]d\mathbf{r}\,d\mathbf{r}' \ . \quad (1)$$

The point is that the integral of the longitudinal response $R_L$ above the inelastic threshold is related to this correlation function through the so-called (inelastic) Coulomb sum rule [9]

$$\int_{\text{inel. thr.}}^{\infty} \frac{R_L(\mathbf{q},\omega)}{[G_E^p(\mathbf{Q}^2)]^2}d\boldsymbol{\omega} = Z\left(1 - \frac{F_E^2(\mathbf{Q}^2)}{[G_E^p(\mathbf{Q}^2)]^2}\right) + c^{(2)}(\mathbf{q}). \quad (2)$$

$\mathbf{q}$ and $\omega$ are the electron momentum and energy transfer to the nucleus and $\mathbf{Q}^2 = \mathbf{q}^2 - \omega^2$. $G_E^p(\mathbf{Q}^2)$ and $F_E(\mathbf{Q}^2)$ are the electric form factors, respectively, of the proton and the nucleus, normalized to 1 at $\mathbf{Q}^2$=0. In the $\mathbf{Q}^2$ range of interest (below 0.5 GeV$^2/c^2$) these form factors are known with an accuracy of a few percent. By determining the Coulomb sum integral one can then extract the proton-proton correlation function. This has been attempted [10] with $(e,e')$ data on $^3$He [11, 12]. However there are limitations which compromise the analysis: (1) The experimental error bars are such that there is actually little information; (2) the integral of the Coulomb sum can be measured up to a maximum energy transfer only; one must then use some extrapolation—for instance an exponential tail—of the integrand to fully evaluate the integral; (3) relativistic corrections should be added [9]; and (4) experimentally the Coulomb sum rule for heavy and medium nuclei has a deficit which, even after corrections of types (2) and (3), is too large to be attributed solely to correlations [13, 14]. It therefore seems possible that there are ill-understood features of the sum rule pertaining even to such light nuclei as $^3$He which prevent the interpretation in terms of correlations.

The most direct measurement of two-body properties will hopefully be provided by threefold coincidence $(e,e'2N)$ experiments [15, 16]. Such experiments will be performed at the new large duty cycle accelerator facilities (Mainz, NIKHEF, MIT/Bates, CEBAF). It is, however, possible to study two-body properties using $(e,e'p)$ experiments: Since the highest momentum components of the nuclear wave function are generated by correlations [7], by measuring them one can study the interaction of two nucleons with small internucleon separations inside a nucleus.

Let us consider the process in which an electron scatters on a proton belonging to a pair of close nucleons [17, 18]. We do not mean that this pair has particularly strong binding or correlation, but just that the scattering occurs at a moment when the two nucleons are close together. In their center of momentum, due to their proximity, these nucleons have large equal and opposite momenta, and to a first approximation we can neglect the momentum of the pair relative to the remaining nucleons. The struck proton is ejected and detected in coincidence with the scattered electron, while the other nucleon of the pair, of mass $M_N$ moves off with the recoil momentum of the reaction, $p_r$; the $A-2$ "spectator" nucleons are at rest. These nucleons, together with the undetected nucleon of the pair, constitute the recoiling system, whose mass is given by

$$M_r^2 = \left[M_{A-2} + \sqrt{M_N^2 + p_r^2}\right]^2 - p_r^2 \ . \quad (3)$$

This expression shows that the recoil mass $M_r$, and consequently the missing energy $E_m = M_r + M_p - M_A$, are only functions of the recoil momentum ($M_p$ is the proton mass, $M_A$ is the target nucleus mass, and $M_{A-2}$ is the mass of $A-2$ spectator nucleon system). In this approximation, therefore, and for a given $p_r$, this process leads to a discrete peak in the continuum missing energy spectrum of the $(e,e'p)$ reaction. When the total momentum of the pair relative to the rest of the nucleus is taken into account, the discrete peak acquires a width and the continuum shows a peak around the previously fixed value of missing energy. The width of this nucleon-nucleon ($N$-$N$) peak will reflect the (initial) momentum distribution of the pair relative to the rest of the nucleus. Its amplitude will reflect the relative wave function of the two nucleons; more precisely the integral over the continuum will give the momentum distribution of the proton in the pair.

We then expect this integral to be compatible with a typical proton momentum distribution (e.g., the nucleon momentum distribution in the deuteron). This can rule out the possibility that the observed structure was generated by a final state interaction (FSI): The correlation that we described between the missing energy and the recoil momentum only signals that the reaction has involved two nucleons while the other nucleons were spectators; such a correlation could then be generated by a FSI (but not with the same amplitude). Specifically the struck nucleon could undergo a final state interaction with one of the other nucleons while the $A-2$ last nucleons are spectators.

This simple picture has already been successfully tested at Saclay on the $^3$He nucleus [19], for recoil momenta between 290 and 515 MeV/$c$. The expected $N$-$N$ peak was observed at the predicted value of the missing energy and the extracted momentum distribution closely resembled that of deuterium. Of course, the fact that an electron can scatter on a pair of nucleons at the moment when they are close together without interacting with the remaining nucleus seems rather natural in $^3$He. This is a loosely bound system, the pair is on average rather distant from the third nucleon (three nucleons for a charge radius of 1.95 fm), and the rescattering should be relatively small, since the $A-2$ system is that of a single nucleon. A question to be answered is whether this description is still valid for more complex and bound nuclei with shorter internucleonic distances.

To settle this question, an experiment on a more dense nucleus is required. To first order in $p_r^2/M_p^2$ the correlation peak is expected at a missing energy

$$E_m = E_{\text{thr}} + \left(\frac{A-2}{A-1}\right)\frac{p_r^2}{2M_p} \ , \quad (4)$$

where $E_{\rm thr}$ is the missing energy corresponding to the continuum threshold. The factor $(A-2)/(A-1)$ is 1/2 for $^3$He, 2/3 for $^4$He, and nearly 1 for medium or heavy nuclei. The contribution of the scattering on a nucleon pair appears at a higher missing energy for the medium and heavy nuclei than for light nuclei, and can overlap real pion production processes.

We have chosen to study $^4$He. It is the simplest nucleus having a binding energy commensurate with heavier nuclei. Its central density 0.18 fm$^{-3}$ is the highest known. Its density exceeds the central density of heavy nuclei by 50% over 17% of its total volume, and the probability of finding two nucleons in $^4$He within 0.5 fm of each other is essentially the same as for heavier nuclei [20]. One might therefore expect the behavior of nucleon pairs inside this nucleus to resemble that inside heavier nuclei. In fact alphalike correlations have been employed [21–23] in modeling nuclei. Yet $^4$He is a relatively simple structure, and realistic calculations of its wave function have become feasible [24–26], although the final continuum state of the $^4$He$(e,e'p)$ reaction can still be only approximated. $^4$He therefore marks a transition between two- and three-body nuclei, for which realistic calculations are possible in both initial and final states of the $(e,e'p)$ reaction, and heavier nuclei, where the relevant many-body problem remains unmanageable at the microscopic level.

The outline of this paper is as follows: The kinematics are described in Sec. II. Section III presents the experimental setup. The data analysis is outlined in Sec. IV. Results are presented and discussed in Sec. V, and conclusions are drawn in Sec. VI.

## II. EXPERIMENTAL SETUP

Our measurements were made at the 720 MeV Linear Accelerator of Saclay using the two magnetic spectrometer setup of the HE1 end station [28]. The "600" spectrometer, of $10^{-3}$ momentum resolution and 40% momentum acceptance, was used to detect the outgoing protons, whereas the "900" spectrometer, of greater resolution ($10^{-4}$) but smaller (10%) momentum acceptance, was used to detect the scattered electrons. The detection package for both spectrometers, which included proportional chambers, plastic scintillator trigger counters, and freon gas Cerenkov counters at atmospheric pressure, enabled an efficient rejection of pions in the electron arm. Two independent microprocessors, one for each spectrometer, read out the wire chamber and the trigger configuration. The experiment could be triggered either on singles, or coincidence events, allowing us to record either type on magnetic tape with little change in the electronic settings. This feature greatly facilitated our $^4$He elastic scattering calibrations. It is worth noting that for coincidence events, a data compression was performed in order to reduce (by a factor of 10) the number of tapes to be replayed off line.

The target was cold, gaseous $^4$He (pressure 10.0 bars, temperature 20.5 K). It was contained in a rectangular box shaped cell (230 mm in the beam direction, 70 mm in the transverse direction, and 70 mm height). Its 50 $\mu$m stainless steel windows were outside the coincidence acceptance of the spectrometers. Target temperature and pressure were read out on line to continuously monitor the density. The $^4$He density decrease due to beam heating was at most 8% at the maximum current (8 $\mu$A), and was monitored accurately by recording the proton singles yields at both low (0.5 $\mu$A) and nominal beam currents. The absolute density was checked repeatedly by measuring the $^4$He elastic cross section against precise measurements of Ref. [29] taken with room temperature targets. In this way we were able to control the (product of) intrinsic detector efficiency, target density, and solid angle to an accuracy of 2%.

The beam current was measured with two nonintercepting toroid beam monitors and a Faraday cup into which the beam was dumped. The difference in their readings, typically 0.5%, set the accuracy of the charge collection. It was also essential to monitor the position and direction of the beam at the target. A split-foil position monitor, close to the target, controlled steering coils to maintain a position stability at the target to better than 0.5 mm.

The extended gas target made it necessary to know the solid angles of both spectrometers for all possible target source points. A special study of the spectrometer properties using a "tracking program" called ORBITE [28] was performed. It showed that for an extended source, both the entry slits and the pole tips determined the solid angle. A parametrization of the relevant cuts applied to particles trajectories was derived [30] to perform very fast computations of the solid angles for single and coincidence cross sections. The variation of solid angle with position along the beam had been checked prior to this experiment using a thin $^{12}$C target that was systematically displaced along the beam.

## III. KINEMATICS

We have measured the cross section of the $^4$He$(e,e'p)R$ reaction for recoil momenta between 225 and 600 MeV/$c$ and for missing energies as high as 160 MeV. This range allows us to encompass the two-body breakup (2bbu) channel where $R$=$^3$H and most of the continuum where $R = d+n$ or $p+n+n$. Our goal was to measure the high momentum components of the $^4$He wave function, which, due to their weakness, required small electron scattering angles $\theta_e$, so that the cross sections remain measurable. Since our maximum electron beam energy was about 700 MeV, the resulting momentum transfer was relatively small, typically 300 MeV/$c$. A high recoil momentum then imply a large ejected proton momentum $p'$ [27, p. 44]. This in turns requires that the electron energy transfer $\omega$ be large and the Bjorken parameter $x_{\rm Bj} \equiv Q^2/(2M_p\omega)$ be small ($x_{\rm Bj}$ <1); such a domain corresponds to the dip region of the inclusive $(e,e')$ response.

In order to minimize $\theta_e$ so as to maximize the counting rate, we detected electrons in the "900" spectrometer, which could be set at $\theta_e$ as low as 25°. In the same vein and to minimize the random coincidence rates, we chose a duty factor of 1% (20 $\mu$s pulses at 500 Hz) with a beam energy of 560 MeV rather than a lower (0.5%) duty

TABLE I. Kinematics of the $(e,e'p)$ reaction on $^4$He. Separate values are given for the 2bbu [$^4$He$(e,e'p)^3$H] and continuum [$^4$He$(e,e'p)R$, $R = d+n$ or $p+n+n$] channels. For the continuum we have tabulated the kinematics corresponding to the missing energy where the peak is expected. All energies are in MeV and all momenta in MeV/$c$.

| Kinematics | 1 | 2 | 3 | 4 | 5 | 6 |
|---|---|---|---|---|---|---|
| incident energy | 559.3 | | | 559.3 | | |
| scattered energy | 400 | | | 360 | | |
| scattering angle | 25° | | | 25° | | |
| momentum transfer | 260.7 | | | 278.3 | | |
| energy transfer | 159.3 | | | 199.3 | | |
| photon-proton angle | 4.2° | 11.9° | 37.9° | 53.9° | 69.9° | 100.6° |
| beam-proton angle | 45° | 45° | 71° | 87° | 103° | 133.8° |
| $\langle i \rangle (\mu$A) | 3.5 | 8.0 | 8.0 | 3.0 | 2.4 | 2.8 |
| | | | 2bbu | | | |
| proton momentum | 507.7 | 575.8 | 559.1 | 542.0 | 521.9 | 481.6 |
| recoil momentum | 248.5 | 308.8 | 379.9 | 439.7 | 499.9 | 599.0 |
| statistics | 1539(46) | 1510(63) | 967(54) | 170(27) | 115(29) | 31.6(15) |
| | | | continuum | | | |
| statistics | 1947(102) | 4222(248) | 4921(236) | 1544(129) | 2035(168) | 737(86) |

factor at the maximum accelerator energy of 700 MeV. This moved our kinematics deeper into the dip region than it would have been at 700 MeV.

The six kinematics settings used in the experiment are presented in Table I. The electron kinematics was kept constant. The recoil momentum was increased from 240 to 600 MeV/$c$ by varying the angle between the outgoing proton and the momentum transfer from 4° to 100°. The range in missing energy required to cover both the 2bbu and the continuum channels adequately was provided by the large acceptance (40%) in the proton momentum $p'$. For the kinematics entries 5 and 6 of Table I, this 40% acceptance was not sufficient to cover the desired range, and two field settings of the proton spectrometer were necessitated. Since the recoil momentum is a sensitive function of $p'$, a strong correlation between the missing energy and the recoil momentum appears within the experimental acceptance; as the missing energy increases, the recoil momentum decreases.

Table I also gives the beam intensity and the number of events measured in each channel. The current was limited to values between 2.4 and 8 $\mu$A due to the low ratio of true coincidences to random coincidences. The statistical accuracy on the cross sections ranges between 4% and 45% for the 2bbu channel, and between 6% and 12% for the integral of the continuum.

## IV. DATA ANALYSIS

The data analysis included the following procedures:

(1) Corrections were made for various counting losses: (a) proton- and electron-trigger dead time losses ($\leq$6% and $\leq$2%, respectively), (b) coincidence trigger losses due to the fact that only one coincidence trigger per beam spill could be handled ($\leq$8.0%), (c) losses due to the rejection of proton triggers separated by less than 470 ns which the "900" drift chambers could not process properly ($\leq$12%) [losses (b) and (c) were very precisely determined using dedicated scalers], (d) track-reconstruction losses from the multiwire proportional chamber system ($\leq$1% and 7% for the proton and electron arms, respectively), and (e) target density losses, determined by comparing data taken at low ($\leq$0.5 $\mu$A) and nominal currents. The overall counting loss could therefore reach 35%. However, the largest corrections [(b) and (c)] were essentially error free, and since we believe the other corrections to be accurate at the 5% relative level, we estimate the error in the experimental rate $n^{\rm expt}_{ee'p}$ to be of the order of 1%. The various correction factors in the different kinematics are tabulated in Table II.

(2) Adjusting the random and coincidence windows in the electron-proton time correlation spectrum. For the analysis of the 2bbu and the integral of the continuum, the allowed window was made asymmetric ($-3$ ns to $+6$ ns), to include those few percent of correlated events for which the timing was slightly wrong (due to the presence of high singles rates in the proton trigger counters).

For the analysis of the continuum in a given missing energy channel we used a smaller symmetric window ($-2$ ns to $+2$ ns) in order to reduce the level of random events. Then we corrected by the proportion of correlated events which lie out of the window because their timing was slightly wrong. This proportion was determined on the whole continuum, since it depends only on the singles rates. The systematic error that might be thus introduced was much smaller than the gain in the statistical error. This improves our knowledge of the shape of the continuum but does not change the integral.

(3) Acceptance determination: For a point target and spectrometers with infinitesimal acceptances in angle and momentum (i.e., infinitesimal phase space for the reaction studied), it is easy to derive the differential cross section $d^6\sigma/dE_{e'}dE_{p'}d^2\Omega_{e'}d^2\Omega_{p'}$ from the yield $n^{\rm expt}_{ee'p}$; this is achieved by dividing the yield by the relevant spectrometer solid angles and energy bites and by the luminosity. This was not quite the case here and the extension of the

TABLE II. Values of the various correction factors. Refer to Sec. IV in the text for explanation of these factors.

| Kinematics | 1 | 2 | 3 | 4 | 5 | 6 |
|---|---|---|---|---|---|---|
| dead time 600 | 0.96 | 0.94 | 0.97 | 0.99 | 0.99 | 0.995 |
| dead time 900 | 0.99 | 0.98 | 0.98 | 0.99 | 0.99 | 0.994 |
| 1 coin/pulse | 0.98 | 0.92 | 0.96 | 0.995 | 0.998 | 0.996 |
| "900" drift chanbers | 0.88 | 0.91 | 0.91 | 0.96 | 0.98 | 0.96 |
| track reconstruction 600 | 0.99 | 0.99 | 0.997 | 0.998 | 0.998 | 0.998 |
| track reconstruction 900 | 0.94 | 0.93 | 0.94 | 0.94 | 0.94 | 0.94 |
| target density | 0.97 | 0.92 | 0.92 | 0.95 | 0.96 | 0.98 |
| total | 0.80 | 0.65 | 0.71 | 0.80 | 0.81 | 0.88 |

experimental phase space had to be taken into account for mainly two reasons:

(a) In the simplest approximation, the plane wave impulse approximation (PWIA), the cross sections can be written as $d^6\sigma/dE_{e'}dE_{p'}d^2\Omega_{e'}d^2\Omega_{p'} = k\sigma_{ep}S(E_m, p_r)$, where $\sigma_{ep}$ is the (off-shell) electron proton cross section, $S(E_m, p_r)$ is the spectral function, and $k$ is a kinematic factor. The cross section then depends sensitively on the recoil momentum $p_r$. Since $p_r$ is not a linear function of the kinematic variables of the detected particles, its average value may differ significantly from its value at the center of the kinematic phase space.

(b) The phase space volume was such that for one kinematics setting, the total $p_r$ "bin width" was about 60 MeV/$c$, allowing nonlinearities of $S(p_r)$ to come into play.

We made a first order analysis by the simple division rule mentioned above. It provided us with an estimate of the curvature of the spectral function in this range of recoil momentum where it had not so far been experimentally measured. We then designed a Monte Carlo simulation of the coincidence apparatus which allowed us to integrate a cross section of the type $k\sigma_{ep}S(E_m, p_r)$ over the full experimental phase space. The previously determined curvature of $S$ was built in the simulation. Only one free parameter entered this simulation: the absolute value of $S$, i.e., the quantity we sought to measure. This parameter was fixed by requiring the equality of the simulated and experimental counting rates $n^{\rm MC}_{ee'p} = n^{\rm expt}_{ee'p}$. This led to the experimental result $S^{\rm expt}$, or equivalently $d^6\sigma^{\rm expt}$. In the limit of infinitesimal phase space, this procedure is equivalent to the extraction of the cross section by the simple division rule.

(4) Radiative corrections: These were made in two steps. We first treated the 2bbu peak at $E_m$=19.8 MeV. With an upper cutoff at $E_m = 19.8 + 4$ MeV, the radiative correction factor varied from 1.33 to 1.36 for the various kinematics; the radiative tail from the 2bbu channel was calculated and subtracted from the continuum cross section. In a second step, in order to deconvolute the continuum, we separated it in several bands in missing energy and we treated each band as a discrete peak. The validity of such an approach was confirmed by the fact that the final result was insensitive to the width of the bands.

A delicate point arose from the noted correlation between the recoil momentum and the missing energy within the acceptance. Without this correlation the radiative tail would decrease smoothly with missing energy. Here this natural decrease with the missing energy is compensated by the cross section increase when the recoil momentum goes down; consequently the 2bbu radiative tail may be more important at large missing energy than near the 2bbu peak. This is especially true for kinematics 5, where the radiative tail of the 2bbu peak amounts to about 30% of the experimental cross section at the largest values of the missing energy.

Finally the systematic error in the 2bbu channel is about 3%, i.e., of the same order as the statistical one for the first two kinematics, and smaller for the other kinematics. For the continuum channel the systematic error is probably slightly larger due to the delicate subtraction of the radiative tail. However, the counting rates in this channel are always very low so that the statistical accuracy cannot be excellent; then the systematic remains negligible relative to the statistical one.

## V. RESULTS

Figure 1 presents the radiatively corrected cross sections as a function of missing energy for our six kinematics, labeled 1–6. The 2bbu peak appears at 19.8 MeV missing energy and the continuum channel extends above the threshold at 26.1 MeV. The numerical values of the cross sections in order of increasing $p_r$ are tabulated in Table III for the 2bbu and in Table IV for the continuum. For the 2bbu the average recoil momentum ranges from 248 MeV/$c$ ("Kin. 1") to 597 MeV/$c$ ("Kin. 6"). For the continuum, as already explained, the average recoil momentum varies with missing energy. We have indicated the average recoil momentum of the whole measured continuum; it ranges from 225 to 487 MeV/$c$.

One can see that as $p_r$ increases the ratio of the 2bbu strength to the integral of the continuum strength decreases; for the larger values of the recoil momentum the continuum clearly dominates the cross section. For point 1 the continuum cross section decreases smoothly with missing energy. For the next two points, a plateau appears, and for the three highest $p_r$ points we observe an increasingly structured shape. We have indicated by an arrow the position where a peak is expected if the cross section were actually dominated by the scattering on a pair of nucleons ($N$-$N$ peak; see the Introduction). For

TABLE III. Experimental cross sections for the $^4$He$(e,e'p)^3$H channel at 19.8 MeV missing energy (2bbu). Errors are statistical only.

| $\theta_{ee'}$ | $\theta_{ep'}$ | $e'$ (MeV) | $p'$ (MeV) | $p_r$ (MeV) | $\frac{d^5\sigma}{d\Omega_{e'}d\Omega_{p'}de'}$ (pb) |
|---|---|---|---|---|---|
| | 45° | 400 | 508 | 248 | 1777 (56) |
| | 45° | 360 | 576 | 309 | 469 (20) |
| | 71° | 360 | 559 | 379 | 187 (11) |
| 25° | 87° | 360 | 542 | 438 | 58.7 (9.4) |
| | 103° | 360 | 522 | 498 | 18.6 (4.7) |
| | 133.8° | 360 | 482 | 597 | 7.7 (3.9) |

points 4–6 ($p_r > 350$ MeV/$c$), a peak appears, and fair agreement is observed between the predicted $N$-$N$ peak and the centroid of the experimental strength. For points 2 and 3 there is less structure. A likely explanation is that, for these smaller momenta ($p_r \approx 300$ MeV/$c$), the scattering on a pair is not fully dominant; other contributions to the strength fill in the low missing energy part of the spectrum and change the expected peak into a plateau.

In Fig. 1, we also show the results of a microscopic calculation of the continuum cross section [31]. This calculation is based on a diagrammatic expansion of the cross section and utilizes a variational wave function [25] calculated with the Argonne potential [32]. It includes final state interactions (FSI's) and meson exchange current (MEC) contributions. The difference between this calculation and one in plane wave impulse approximation (PWIA) is small. The calculation predicts the scattering on a pair of nucleons to be indeed the dominant process; the contribution of MEC never exceeds 25%.

The calculation for points 4–6 of Fig. 1 agrees well with the data. For point 3 it predicts a cross section

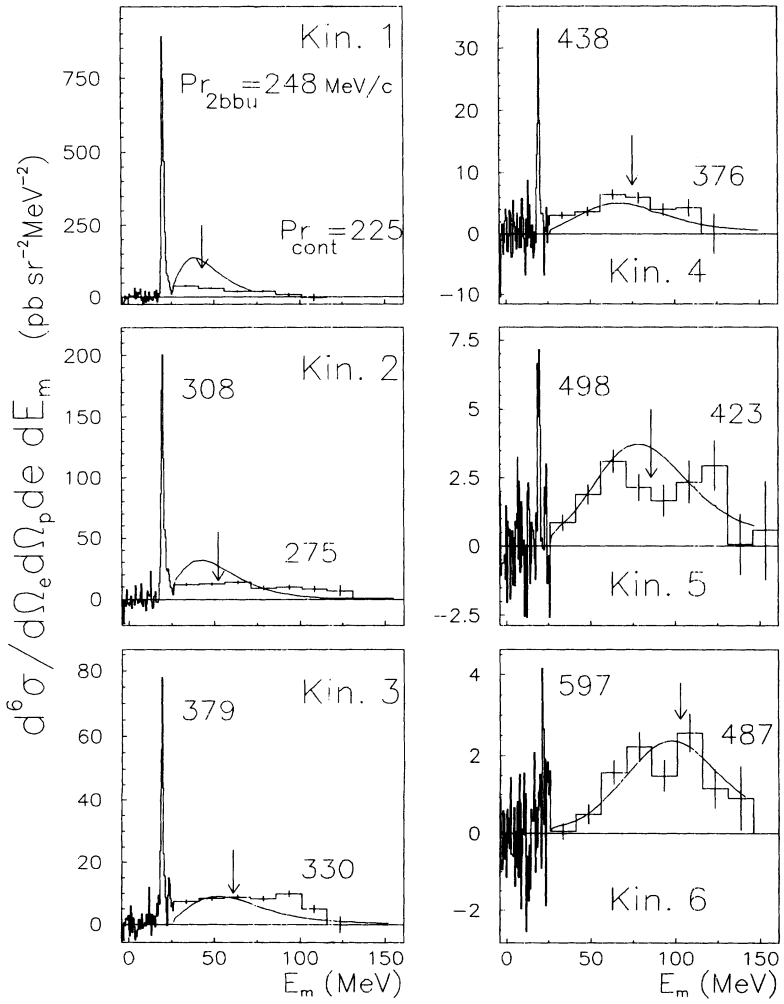


FIG. 1. Radiatively corrected experimental cross section versus missing energy. The arrow indicates where the $N$-$N$ peak is expected. The curves are the result of a microscopic calculation based on a diagrammatic expansion of the cross section [31].

approaching zero at the continuum threshold. This is not consistent with the data and the discrepancy cannot be attributed to insufficient missing energy resolution; the latter, measured on the 2bbu peak, is $\approx$ 0.5 MeV, much smaller than the 6 MeV which separates the 2bbu from the continuum threshold. A similar remark holds for point 2, but here we also note that the theory considerably exceeds the data. For point 1 the discrepancy appears even larger. The calculation appears to be successful for high recoil momentum where the cross section is dominated by the scattering on nucleon pairs. For intermediate recoil momentum this process is probably no longer dominant, and it can be the reason for the large discrepancies with the data.

In the PWIA one can extract the momentum distribution of the continuum by dividing the cross section by the elementary off-shell proton cross section $\sigma_{ep}$, and integrating over the missing energy acceptance. In order to account for reaction mechanism effects not included in the PWIA we multiply the momentum distribution extracted assuming the PWIA by a correction factor. This factor is the ratio of the integral of the theoretical cross sections calculated in the PWIA to the same integral for the full (PWIA+FSI+MEC) calculation:

TABLE IV. Experimental cross sections for the continuum channel, $^4$He$(e,e'p)R$. Errors are statistical only.

| No. Kin. | $\theta_{e'}$ (deg) | $\theta_{p'}$ (deg) | $e'$ (MeV) | $p'$ (MeV/$c$) | $E_m$ (MeV) | $p_r$ (MeV/$c$) | $\frac{d^6\sigma}{d\Omega_{e'}d\Omega_{p'}de'dE_m}$ (pb MeV$^{-2}$ sr$^{-2}$) |
|---|---|---|---|---|---|---|---|
| | | | 400 | 483 | 33.5 | 223 | 38.2 (2.6) |
| | | | 400 | 454 | 48.5 | 195 | 30.5 (2.7) |
| 1 | 25.2 | 45 | 400 | 423 | 63.5 | 164 | 19.8 (2.9) |
| | | | 396 | 399 | 78.5 | 140 | 20.4 (3.4) |
| | | | 388 | 383 | 93.5 | 123 | 8.3 (4.9) |
| | | | 360 | 554 | 33.5 | 287 | 11.8 (1.16) |
| | | | 360 | 529 | 48.5 | 263 | 12.3 (1.27) |
| | | | 360 | 502 | 63.5 | 237 | 13.7 (1.41) |
| 2 | 25 | 45 | 360 | 474 | 78.5 | 210 | 9.1 (1.54) |
| | | | 360 | 445 | 93.5 | 182 | 9.7 (1.74) |
| | | | 354 | 426 | 108.5 | 164 | 8.28 (2.27) |
| | | | 345 | 413 | 123.5 | 153 | 6.76 (4.16) |
| | | | 360 | 537 | 33.5 | 361 | 7.26 (0.62) |
| | | | 360 | 512 | 48.5 | 339 | 8.31 (0.69) |
| | | | 360 | 486 | 63.5 | 316 | 8.70 (0.78) |
| 3 | 25 | 71 | 360 | 458 | 78.5 | 293 | 8.24 (0.86) |
| | | | 360 | 429 | 93.5 | 270 | 9.82 (1.00) |
| | | | 353 | 411 | 108.5 | 262 | 4.99 (1.32) |
| | | | 360 | 520 | 33.5 | 421 | 3.11 (0.60) |
| | | | 360 | 495 | 48.5 | 400 | 3.67 (0.69) |
| | | | 360 | 469 | 63.5 | 379 | 6.47 (0.80) |
| 4 | 25 | 87 | 360 | 441 | 78.5 | 357 | 5.96 (0.90) |
| | | | 359 | 414 | 93.5 | 337 | 4.06 (1.01) |
| | | | 353 | 394 | 108.5 | 328 | 4.29 (1.38) |
| | | | 360 | 500 | 33.5 | 481 | 0.85 (0.30) |
| | | | 360 | 476 | 48.5 | 461 | 1.88 (0.36) |
| | | | 360 | 449 | 63.5 | 440 | 3.10 (0.42) |
| | | | 360 | 422 | 78.5 | 418 | 2.14 (0.49) |
| 5 | 25 | 103 | 360 | 393 | 93.5 | 396 | 1.65 (0.60) |
| | | | 360 | 361 | 108.5 | 372 | 2.34 (0.78) |
| | | | 360 | 326 | 123.5 | 348 | 2.94 (0.93) |
| | | | 359 | 290 | 138.5 | 326 | 0.06 (1.11) |
| | | | 351 | 267 | 153.5 | 321 | 0.58 (1.80) |
| | | | 360 | 460 | 33.5 | 580 | 0.05 (0.20) |
| | | | 360 | 436 | 48.5 | 559 | 0.49 (0.25) |
| | | | 360 | 410 | 63.5 | 537 | 1.57 (0.31) |
| | | | 360 | 383 | 78.5 | 513 | 2.22 (0.36) |
| 6 | 25 | 133.8 | 360 | 354 | 93.5 | 489 | 1.48 (0.41) |
| | | | 360 | 323 | 108.5 | 464 | 2.56 (0.47) |
| | | | 359 | 291 | 123.5 | 439 | 1.16 (0.52) |
| | | | 351 | 271 | 138.5 | 431 | 0.91 (0.83) |

$$n_{\text{continuum}}(p_r) = \left[\frac{\int d^6\sigma^{\text{PWIA}} dE_m}{\int d^6\sigma^{\text{PWIA+FSI+MEC}} dE_m}\right] \times \int \frac{d^6\sigma}{\sigma_{ep}} dE_m \ . \quad (5)$$

For the off-shell proton cross section we chose the "cc1" prescription by De Forest [33] since it is relativistic and gauge invariant. Note that this expression implies that the momentum distribution is normalized so that $\int_0^\infty 4\pi p^2 n(p) dp = Z = 2$. Since we believe the continuum cross section to be dominated by the scattering on a pair of nucleons, this momentum distribution is essentially the momentum distribution of one of the nucleons of a pair of nucleons inside a $^4$He nucleus. In order to compare it to its equivalent in the case of a free pair, i.e., the deuteron momentum distribution, we must divide it by a factor of 3 to account for the fact that there are three $n$-$p$ pairs in isospin state $T = 0$ in the $^4$He nucleus. There are actually four $n$-$p$ pairs, but due to a combination of selection rules and kinematic arguments the contributions from the $T = 1$ pairs are negligible in our kinematics, as is the contribution from the $p$-$p$ or $n$-$n$ pairs [34].

In Fig. 2 we compare the continuum momentum distributions of $^4$He and $^3$He (renormalized by the number of $T = 0$ pairs) to the deuterium momentum distribution (the number of pairs in isospin state $T = 0$ is 3/2 in $^3$He). For the high recoil momenta of this experiment, the three distributions appear very similar. This feature validates the hypothesis that the cross section is generated by scattering on the high momentum part of nucleon pairs and not by FSI's and it indicates that the wave function of nucleon pairs is hardly disturbed by the nuclear medium, even in the case of the relatively dense $^4$He nucleus.

Figure 3 presents our data in the 2bbu channel, again with Laget's diagrammatic calculation. The data show a strong disagreement with the PWIA calculation. FSI and MEC calculations can explain a part of the discrepancy, but there remains a factor 3–4 to explain. One may be surprised that the calculation is more successful for the continuum than the 2bbu channel. This may be understood by noting that the continuum is dominated by a well-determined process: the plane wave scattering on a pair of nucleons. On the other hand the 2bbu channel in the PWIA is purely $S$ wave, with a zero around 450 MeV/$c$. In this region, large momenta must be generated by complex mechanisms such as final state interactions and meson exchanges.

To our knowledge there is no other data for the continuum, but for the 2bbu channel there are data from NIKHEF [35, 36]. Two sets of kinematics are included in these data, one for recoil momenta 0–200 MeV/$c$, the other for recoil momenta 100–340 MeV/$c$. Figure 4 presents the momentum distribution extracted in the PWIA from the NIKHEF data and from our kinematic points 1–3. If the PWIA were valid, they should be identical. We first note that in the region of overlap there are

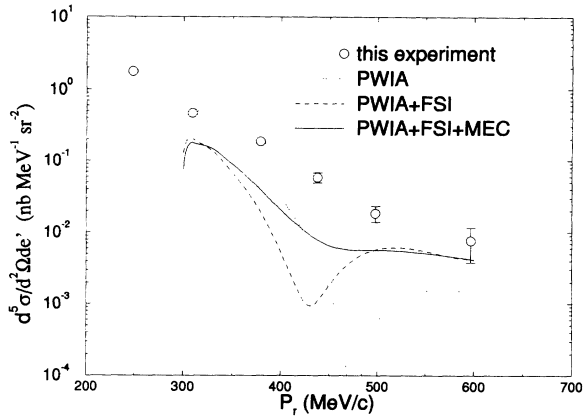


FIG. 3. Radiatively corrected cross section in the 2bbu channel. The curves are the result of a microscopic calculation based on a diagrammatic expansion of the cross section [31].

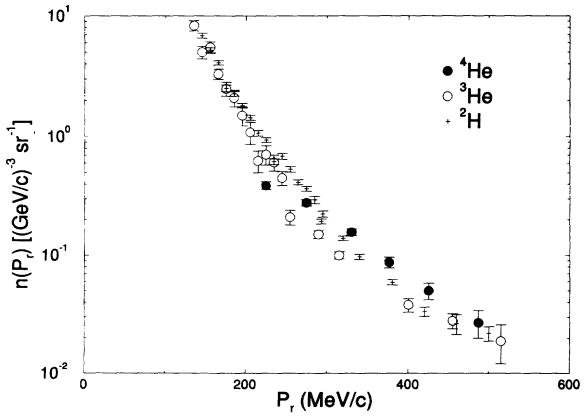


FIG. 2. Momentum distribution after corrections for extra PWIA reaction mechanisms and normalized to the number of $T = 0$ $p$-$n$ pairs. The continuum of $^4$He (this experiment) and $^3$He [38, 19] are presented together with the 2bbu of deuterium [39, 40].

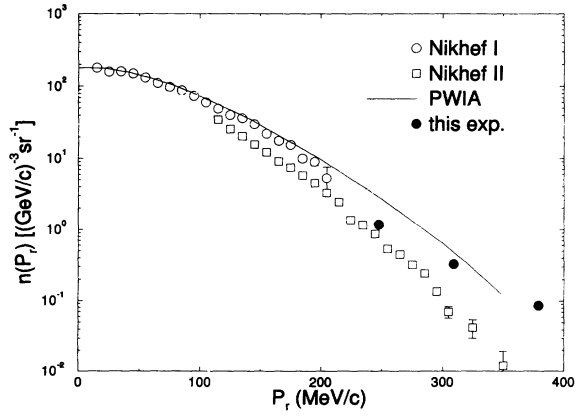


FIG. 4. 2bbu channel: comparison of our first three kinematics with NIKHEF data [35]. The momentum distribution extracted in the PWIA (cross section divided by the cc1 prescription for $\sigma ep$) is presented. The curve is a variational calculation [25] with the Urbana potential [37].

important differences between the two NIKHEF (I and II) kinematics, indicating that non-PWIA contributions are important. Our data appear between the NIKHEF-II data and a PWIA calculation based on a variational wave function [25] derived with the Urbana potential [37]. The difference between the two sets of data illustrates again the importance of extra-PWIA effects in the 2bbu channel for high recoil momenta. The two experiments were performed at about the same momentum transfer (250 MeV/$c$ at NIKHEF and 280 MeV/$c$ at Saclay) but the energy transfer was different (102 MeV and 200 MeV, respectively), as was the kinetic energy in the proton+triton center of mass (75 MeV and 170 MeV). With our larger energy transfer, our kinematics have smaller $x_{\rm Bj}$ values than those of NIKHEF ($x_{\rm Bj} = Q^2/2M_p$); they plunge deeper into the "dip" region where uncertainties in describing the reaction mechanisms are substantial.

## VI. SUMMARY AND CONCLUSION

Our goal was to study the high momentum components of nucleons in $^4$He, and in particular to test the idea that they were generated by nucleon pairs, as had been done in an earlier $(e,e'p)$ experiment [19] for the simpler and less dense $^3$He nucleus. To this end we measured the $^4{\rm He}(e,e'p)R$ cross sections as a function of missing energy for recoil momenta between 225 and 600 MeV/$c$. Our results show that the $(e,e'p)$ reaction at recoil momenta greater than $\approx$ 350 MeV/$c$ is dominated by the scattering on a pair of nucleons:

On the one hand, there is kinematic evidence. Our spectra exhibit a structure which shifts with recoil momentum and whose centroid appears at a missing energy consistent with the scattering on such a pair. The prominence of the observed structure increases as the recoil momentum increases. Its width (at higher missing momenta) reflects the momentum of the center of mass of the pair relative to the remaining nucleus.

Second, the magnitude of the cross section is a dynamical evidence that we observe scattering from one of a pair of nucleons and not FSI's. For recoil momenta above 300 or 350 MeV/$c$ agreement is found between the data and a microscopic theory which predicts the reaction to occur predominantly on interacting nucleon-nucleon pairs; on the other hand, the amplitude is too large to be generated by FSI's alone. Furthermore, the continuum momentum distribution, for the high recoil momenta of this experiment, appears to be very similar to that of deuterium. The high momentum part of the wave function of two nucleons seems to be something universal and indepenent of a possible surrounding nuclear medium.

The characteristics of our yield therefore possess the signature of the scattering on a one of a pair of nucleons. Such high momentum components do not exist in an independent particle shell model. Therefore they can be said to be induced by nucleon-nucleon correlations, and at short range since at high momentum.

In contrast the cross section in the 2bbu channel is considerably underestimated by theory. In the PWIA there is very little strength in the 2bbu channel and the actual cross section is dominated by complex reaction mechanism effects.

These data were taken at low momentum transfer and at small electron scattering angles, i.e., for predominantly longitudinal kinematics. For this reason, the contribution of mesonic effects should be weak. Nevertheless, it would be interesting to perform this kind of experiment in other kinematic regions, and especially in the quasielastic $x_{\rm Bj} \approx 1$ region where the reaction mechanism is better understood. At energies below 1 GeV there may be a small kinematic domain for this; the condition is that one can detect the electron and the proton on the same side of the beam line [27, p. 44], which was not the case at the ALS. At higher energies (a few GeV) there is no kinematical limitation for performing the experiment in the quasielastic region. Note, however, that one will then probably have to face the complication occurring from relativistic effects.

Another point is that, at these energies, a decomposition of the structure functions for the cross section in the domain of large recoil momenta, missing energies, and momentum transfers will hopefully be performed. This should considerably elucidate features of the $(e,e'p)$ reaction mechanism until now inextricable. As a first step in this direction we have performed a $T/L$ separation of the $^3{\rm He}(e,e'p)R$ cross section at 260 MeV/$c$ recoil momentum; we will report on this experiment elsewhere.

## ACKNOWLEDGMENTS

We would like to thank Jean-Marc Laget for his contribution to the execution and analysis of this work. The work of M.K.B. was supported in part by the U.S. National Science Foundation.

[1] T. Berggren and H. Tyren, Annu. Rev. Nucl. Sci. **16**, 153 (1966).
[2] B. Frois and C. Papanicolas, Annu. Rev. Nucl. Part. Sci. **37**, 133 (1987).
[3] J. Mougey *et al.*, Nucl. Phys. **A262**, 461 (1976).
[4] R.W. Lourie *et al.*, Phys. Rev. Lett. **56**, 2364 (1986).
[5] P.E. Ulmer *et al.*, Phys. Rev. Lett. **59**, 2259 (1987).
[6] N. d'hose *et al.*, Phys. Rev. Lett. **63**, 859 (1989).
[7] K. Gottfried, Ann. Phys. (N.Y.) **21**, 29 (1963).
[8] R.D. Viollier and J.D. Walecka, Acta Phys. Pol. B **8**, 25 (1977).
[9] T. De Forest, Jr., Nucl. Phys. **A414**, 347 (1984).
[10] D.H. Beck, Phys. Rev. Lett. **64**, 268 (1990).
[11] C. Marchand *et al.*, Phys. Lett. **153B**, 29 (1985).
[12] K. Dow *et al.*, Phys. Rev. Lett. **61**, 1706 (1988).
[13] J. Morgenstern *et al.*, Nucl. Phys. **A446**, 315c (1985).
[14] A. Zghiche *et al.*, Nucl. Phys. **A572**, 513 (1994).
[15] Y.N. Srivastava, Phys. Rev. **135**, B612 (1964).

[16] U.L. Yu, Ann. Phys. (N.Y.) **38**, 392 (1966).
[17] L. Frankfurt and M. Strikman, Phys. Rep. **76**, 236 (1981).
[18] J.M. Laget, Nucl. Phys. **A358**, 275 (1981).
[19] C. Marchand *et al.,* Phys. Rev. Lett. **60**, 1703 (1988).
[20] Y. Akaishi, Int. Rev. Nucl. Phys. **4**, 259 (1986).
[21] A. Arima and V. Gillet, Ann. Phys. (N.Y.) **66**, 117 (1971).
[22] R.J. Turner and A.D. Jackson, Nucl. Phys. **A192**, 200 (1972).
[23] H. Horiuchi and K. Ikeda, Int. Rev. Nucl. Phys. **4**, 1 (1986).
[24] Y. Akaishi, Nucl. Phys. **A416**, 409c (1984).
[25] R. Schiavilla, V.R. Pandharipande, and R.B. Wiringa, Nucl. Phys. **A449**, 219 (1986).
[26] R. Schiavilla, Phys. Rev. Lett. **65**, 835 (1990), and private communication.
[27] J.M. Le Goff, Ph.D. thesis, Université Paris Sud, 1991.
[28] Ph. Leconte *et al.,* Nucl. Instrum. Methods **169**, 401 (1980).
[29] C.R. Ottermann, Nucl. Phys. **A436**, 688 (1985).
[30] J.M. Le Goff and P. Vernin, rapport de stage CEA, 1987.
[31] J.M. Laget, in *New Vistas in Electronuclear Physics,* edited by E. Tomusiak *et al.* (Plenum, New York, 1986), p. 361.
[32] R.B. Wiringa, R.A. Smith, and T.L. Ainsworth, Phys. Rev. C **29**, 1207 (1984).
[33] T. De Forest, Jr., Nucl. Phys. **A392**, 232 (1983).
[34] J.M. Laget (private communication).
[35] J.F.J. Van Den Brandt *et al.,* Phys. Rev. Lett. **60**, 2006 (1988).
[36] J.F.J. Van Den Brandt *et al.,* Phys. Rev. Lett. **66**, 409 (1991).
[37] I.E. Lagaris and V.R. Pandharipande, Nucl. Phys. **A359**, 331 (1981).
[38] E. Jans *et al.,* Nucl. Phys. **A475**, 687 (1987).
[39] M. Bernheim *et al.,* Nucl. Phys. **A365**, 349 (1981).
[40] S. Turk-Chieze *et al.,* Phys. Lett. **142B**, 145 (1984).